Theoretical Chemistry Accounts (2021) 140:90
https://doi.org/10.1007/s00214-021-02792-3

REGULAR ARTICLE

Quantum chemical investigation of the ground- and excited-state acidities of a dihydroxyfuranoflavylium cation

Jing Cui[1] · Farhan Siddique[1] · Reed Nieman[2] · Gustavo T. M. Silva[3] · Frank H. Quina[3] · Adelia J. A. Aquino[1,4,5]

Received: 3 April 2021 / Accepted: 4 June 2021 / Published online: 14 June 2021
© The Author(s), under exclusive licence to Springer-Verlag GmbH Germany, part of Springer Nature 2021

Abstract

The two hydroxyl groups of the 4′,7-dihydroxyfurano-3,2′-flavylium cation (**1**), a synthetic analog of the aurone pigments of plants, have been shown to have different relative acidities in the ground state (S_0) and the lowest excited singlet state (S_1). In the ground state, the 4′-OH group is slightly more acidic, while in the excited state, the molecule is strongly photoacidic and deprotonation occurs preferentially from the 7-OH group. In order to compare the relative acidities of these two OH groups via quantum chemical methodology, a common reference state was employed in which an explicit water molecule was hydrogen-bonded to each of the OH groups of 1. The relative acidities of the two OH groups were then inferred from the differential change in energy along the coordinate for proton transfer to the explicit water molecule via time-dependent density functional calculations (B3-LYP with Grimme's D3 dispersion correction; TZVP basis set; and PCM to simulate an aqueous environment). The calculated acidity changes confirm the experimentally observed inversion in the relative acidities between S_0 and S_1. The enhanced photoacidity of S_1 was also mirrored in the natural transition orbitals and the decrease in the negative change on the oxygen atoms of the OH groups. Employing a common reference state with an explicit water as the proton acceptor should thus serve as a convenient strategy for exploring the relative ground- and excited-state acidities of the OH groups of natural or synthetic dyes, especially when the values are not readily accessible through experiment.

Keywords Anthocyanins · Flavylium cation · DFT · Excited-state proton transfer

1 Introduction

Anthocyanins are the primary natural pigments responsible for most of the red, blue and purple colors of flowers, fruits and leaves [1–3]. Anthocyanin and many of their synthetic flavylium cation analogs have a complex pH-dependent chemistry [1–8]. Thus, at strongly acidic pH, the exclusive form is the visibly colored flavylium cation form. At pH values above ca. pH 3, attack of water on the flavylium cation can result in formation of the near colorless hemiketal form that can then undergo ring-opening tautomerism to the corresponding near colorless chalcones. In hydroxyflavylium cations, deprotonation to form the neutral conjugate base form of the flavylium cation contributes an additional equilibrium to the multiequilibrium system. In the lowest excited singlet state, natural anthocyanins and synthetic hydroxyflavylium and pyranoflavylium cations are strong photoacids, undergoing ultrafast adiabatic excited-state proton transfer (ESPT) to water on a picosecond time scale [8–10].

Among the molecular ancestors of anthocyanins, the aurones, which are responsible for the yellow color of some flowers, possess an additional furan ring in their molecular structure (Scheme 1). Recently, synthetic furanoflavylium analogs of aurones have been shown to exhibit similar multistate equilibria to those of anthocyanins and synthetic flavylium cations [11, 12]. Particularly interesting are the acid–base properties of the ground and lowest excited singlet states of the 4′,7-dihydroxyfurano-3,2′-flavylium cation (**1**)

✉ Adelia J. A. Aquino
quina@usp.br; adelia.aquino@univie.ac.at

1 School of Pharmaceutical Science and Technology, Tianjin University, Tianjin 300072, People's Republic of China

2 Department of Chemistry and Chemical Biology, University of New Mexico, Albuquerque, NM 87131, USA

3 Instituto de Química, Universidade de São Paulo, Av. Lineu Prestes 748, São Paulo, SP 05508-030, Brazil

4 Department of Mechanical Engineering, Texas Tech University, Lubbock, TX 79409, USA

5 Institute for Soil Research, University of Natural Resources and Life Sciences, Vienna, Peter-Jordan-Strasse 82, 1190 Vienna, Austria

Scheme 1 Structures of the compounds

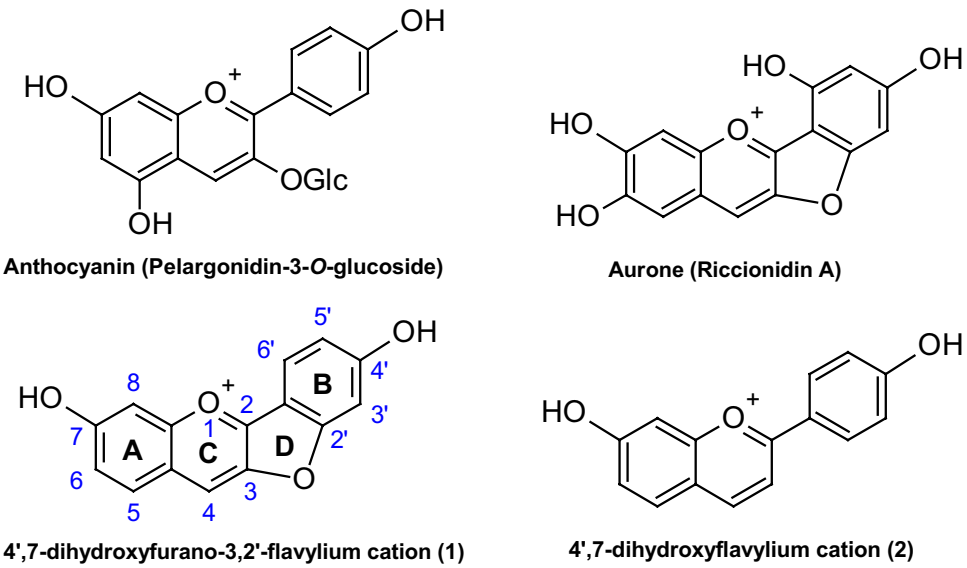

in aqueous solution. Thus, unlike the analogous 4′,7-dihydroxyflavylium cation (**2**), in which the 7-hydroxy group is ca. 1 pK unit more acidic than the 4′-OH group in the ground state, compound **1** was found to deprotonate preferentially at the 4′-OH group in the ground state (Scheme 1). In contrast, in the lowest excited singlet state, the ESPT to water occurred preferentially from the 7-OH group [11].

Given the complexity of much of the chemistry of these natural plant pigments and their synthetic analogs, there is a growing interest in the development of computational quantum chemical methodological approaches for the rationalization and prediction of the ground and excited state properties of dyes or pigments related to anthocyanins, pyranoanthocyanins and their synthetic analogs [13–19]. Knowledge of this type is particularly important for tailoring or adapting the structure in order to optimize the color, stability and properties for a given potential application. In the present work, we report a straightforward and expeditious quantum chemical approach for comparing the relative acidities of OH groups of pigments of this type in both the ground and singlet excited state. The approach is tested by calculations on compound **1** that verify both the strongly enhanced acidity of the excited state and the experimentally observed [12] inversion in the ground- and excited-state acidities of the 4′-OH and 7-OH groups of the furanoflavylium cation **1**.

2 Computational details

Density functional theory (DFT) was used for the characterization of stationary points and potential energy curve pathways of the proton detachment from the hydroxyl groups of the compounds in both the ground (S_0) and first excited singlet (S_1) states. For the DFT calculations, the widely used the hybrid exchange-correlation functional B3-LYP [20] was employed with the D3 dispersion correction of Grimme [21]. The basis set TZVP [22, 23] was used in all calculations. The Gaussian09 [24] program suite was used to perform the calculations. The non-specific effects of the polar solvent environment were simulated using the polarizable continuum model (PCM) [25, 26] implemented using the self-consistent reaction field (SCRF) [25, 27] approach in Gaussian09. The wave function analysis program TheoDORE [28, 29] was used for the natural transition orbital (NTO) [30] analysis.

Initially, the ground-state structures of the isolated systems were fully optimized by means of the B3-LYP/TZVP approach. The first singlet excited state of the furanoflavylium was optimized using TD-DFT with the same functional taking the corresponding optimized geometry of S_0 as the starting point for the S_1 calculations. The potential curves for proton transfer to a single water molecule were computed in the polar environment by stepwise elongation of the O–H bond of the hydroxyl group of interest in 0.1 Å increments using the same method employed for the calculation of the stationary points. All structures were reoptimized using water as a polar environment with the dielectric constant of 78.39. The theoretical absorption spectrum was calculated from the vertical excitation energies (E_i) for the first 10 excited states and the corresponding oscillator strengths (f_i) employing, as in previous work [18, 19], as a sum of superimposed Gaussian functions centered on each E_i [31]:

$$\varepsilon(\bar{\nu}) = 26954 \sum_i \left(\frac{\mathrm{f}_i}{\Delta_{1/2}} \right) \exp\left[-2.733 \left(\frac{E - E_i}{\Delta_{1/2}} \right)^2 \right] \quad (1)$$

where $\Delta_{½}$ is the spectral bandwidth (full width at half maximum) in eV, assumed to be 0.36 eV, and $\varepsilon(\bar{\nu})$ is the molar

absorption coefficient in units of M^{-1} cm^{-1}. The published absorption spectrum [12] was digitized with the online application WebPlot Digitizer [32].

3 Results and discussion

The starting point for our calculations on the furanoflavylium cation **1** was the adoption of a common reference state for the two OH groups of the molecule. This reference state was constructed by hydrogen bonding each of the two OH groups to an explicit water of hydration, followed by minimization of the geometry in a continuum aqueous-like medium (Fig. 1). In addition to creating a common initial reference state against which to compare the acidity of the two OH groups, the specific water molecules served as discreet proton acceptors, found to be necessary in prior computational studies to reproduce experimental acidity trends. Employing a single discrete water molecule as the proton acceptor rather than a larger water cluster proved, in preliminary calculations, to be a necessary expedient due to complications in maintaining entirely equivalent water clusters hydrogen-bonded to the two OH groups during geometry optimization.

The B3-LYP/TZVP energies for the 10 lowest excited singlet states of the furanoflavylium cation **1** with the two discrete water molecules in a PCM aqueous environment (Table 1) were employed to construct the theoretical absorption spectrum. As shown in Fig. 2, the theoretical spectrum based on overlapping Gaussians with a bandwidth of 0.36 eV agrees satisfactorily with the experimental spectrum reported in water at pH 1 [12] over virtually the entire UV–visible spectrum. The hole (occupied) and particle (virtual) components of the natural transition orbitals (NTOs) [30] associated with the transition to the first excited singlet state (S_1), depicted in Fig. 3, are dominated by the HOMO and LUMO, respectively, as is generally the case for flavylium cations.

By employing a common reference state for the two OH groups, the relative acidities of the two OH groups of the molecule can be rather straightforwardly inferred by

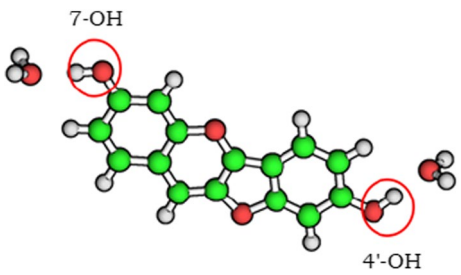

Fig. 1 B3-LYP/TZVP optimized structure of the 4′,7-dihydroxy-3,2′ furanoflavylium cation **1** with two discrete water molecules in a PCM aqueous environment. Atom color code: green—C; red—O; grey—H

Table 1 B3-LYP/TZVP/PCM vertical excitation energies and the corresponding oscillator strengths for the 10 lowest excited singlet states of the furanoflavylium cation **1** with the two discrete water molecules in a PCM aqueous environment

State	ΔE (eV)	Oscillator strength
S_1	2.824	0.8551
S_2	3.336	0.1752
S_3	3.588	0.0099
S_4	4.071	0.0143
S_5	4.768	0.1228
S_6	4.880	0.0071
S_7	5.181	0.0026
S_8	5.349	0.4548
S_9	5.410	0.1493
S_{10}	5.533	0.0001

comparing the relative change in the energy of the molecule upon increasing the O–H distance of either the hydrated 4′-OH group or the hydrated 7-OH group, derived from TD-DFT calculations on the system. Figure 4 shows the difference between the two OH groups, as the relative change in energy in dimensionless units (= ΔE(in eV)/0.059 V), in the ground state and in the lowest excited state of compound **1** when only the 4′-OH bond or only the 7-OH bond was selectively stretched. All structures were reoptimized for each fixed O–H distance, using water as a polar environment. In the ground state, this difference should asymptotically approach ΔpK_a, i.e., the differences between the pK_as of the two OH groups upon complete proton transfer to water, and, for the excited singlet state, the value of ΔpK_a* for ESPT.

The upper curve in Fig. 4 corresponds to the dimensionless energy difference between stretching the 7-OH or the 4′-OH bond along the coordinate for proton transfer to water in the ground state, i.e., [E(7-OH)-E(4′-OH)]/0.059 V. The denominator (0.059 V) is the Nernst´s law change in

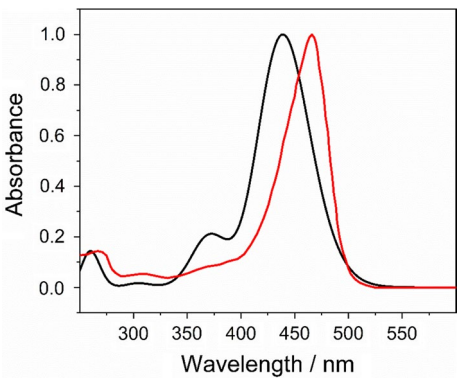

Fig. 2 Comparison of the B3-LYP/TZVP/PCM predicted absorption spectrum (red curve) with the normalized experimental spectrum [12] at pH 1 in water (black curve)

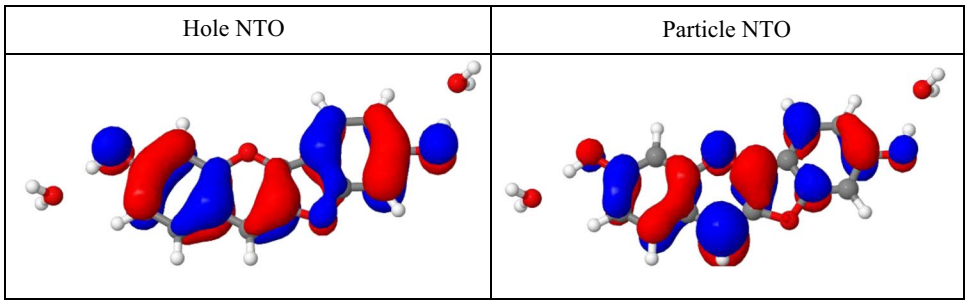

Fig. 3 The NTO hole/particle pair for the S_1 state of the furanoflavylium cation **1** with two discrete water molecules in an aqueous environment. B3LYP/TZVP/PCM calculations. Isovalue = ±0.03 *e*/Bohr^3

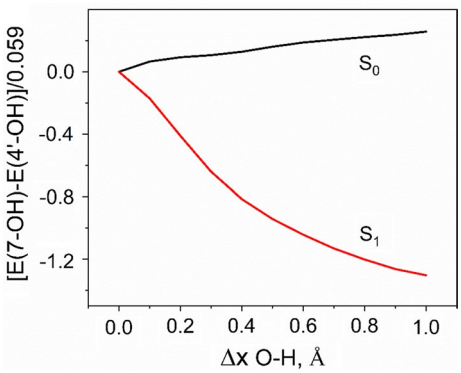

Fig. 4 Difference in the potential energy as a function of stretching (Δx) of only the 7-OH bond compared to that stretching only the 4′-OH bond in the ground state (black curve) or in the lowest excited singlet state (red curve), expressed as $[E(7-\mathrm{OH})-E(4'-\mathrm{OH})]/0.059\mathrm{V}$

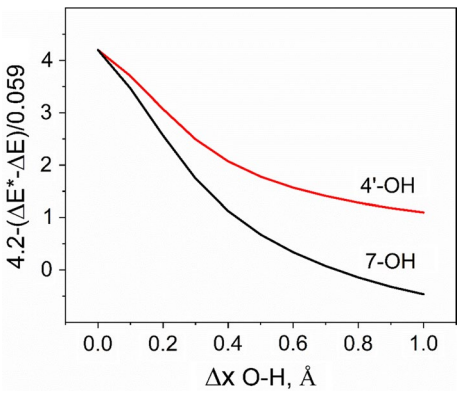

Fig. 5 Difference between the potential energy changes in the lowest excited singlet state (ΔE^*) and in the ground state (ΔE) relative to the equilibrium geometry for selective stretching of either the 4′-OH bond (black curve) or the 7-OH bond (red curve), expressed as $4.2-(\Delta E^*-\Delta E)/0.059$, i.e., taking the ground state pK_a of 4.2 as the reference point

potential for a unit change in the pH, which converts the calculated energy difference into a ΔpK_a value. The positive trend of the curve clearly indicates that the energy increases more rapidly along this coordinate for the 7-OH bond than for the 4′-OH group, i.e., that the 4′-OH group is slightly more acidic of the two. Although the value of ΔpK_a that can be inferred from the trend of the curve is not large, only ca. 0.3–0.4 pK units, it is clearly in line with the experimental data pointing to the greater acidity of the 4′-OH group. In contrast, the lower curve, which corresponds to the analogous energy difference in the lowest excited singlet state, S_1, shows that ESPT from the 7-OH group to water is favored over that from the 4′-OH group by more than 1 pK* unit. This approach appears to be more sensitive to differences in acidity than a simple comparison of a parameter such as the natural charges on the oxygen atoms of the two OH groups. Thus, for the ground state, the two natural charges on these oxygens are found to be the same (-0.638 *e*). Nonetheless, in line with the increased acidity of the lowest excited singlet state, both natural charges decrease in S_1, with the 4´-OH oxygen atom slightly more negative than the 7-OH oxygen atom (− 0.606 *e* vs. 0.596 *e*, respectively).

Figure 5 compares the changes in the calculated ground- and excited-singlet-state energies, relative to the energy of the corresponding equilibrium geometries, along the coordinate for proton transfer to water for each of the two OH groups of the furanoflavylium cation **1**. Taking the experimental ground state pK_a in water of 4.2 as the reference point, the predicted value of pK_a* for ESPT from the 4′-OH group is of the order of 1, while the 7-OH group is predicted to be between ca. − 0.5 and − 1. This latter value is in reasonable agreement with the experimental value of pK_a* of ca. − 0.1 for the 7-OH group derived from the analysis of the pH dependence of the picosecond time-resolved fluorescence decay of the furanoflavylium **1**.

4 Conclusions

The adoption of a common reference state with an explicit water molecule hydrogen-bonded to each of the two OH groups of the furanoflavylium cation **1** permits inferences about the relative acidities of the two OH groups via expeditious TD-DFT calculations along the coordinate for proton transfer to the explicit water molecule. The calculated results for the relative acidities agree with the experimental finding

[12] that there is an inversion in the relative acidities of the two OH groups in going from the ground to the excited singlet state (S_1). Moreover, the NTOs (Fig. 3) for the S_1 state clearly point to the origin of the enhanced photoacidity of S_1 compared to the ground state. Thus, the electronic excitation results in a significant shift of the electron density from the A and B rings and the oxygen atoms of the attached OH-groups into the C-ring upon electronic excitation. This strategy of employing a common reference state with an explicit water as the proton acceptor should serve as a convenient approach for natural or synthetic dyes with multiple OH groups, especially when the relative acidities are not readily accessible through experiment.

Acknowledgements We are grateful for generous support by the School of Pharmaceutical Science and Technology, Tianjin University, China, including computer time on the SPST computer cluster Arran. The authors in Brazil thank INCT-Catálise (CNPq 465454/2014-3; 444061/2018-5) and NAP-PhotoTech for support, the CNPq for a research productivity fellowship (F.H.Q.) and the Coordenação de Aperfeiçoamento de Pessoal de Nível Superior—Brasil (CAPES)—Finance Code 001—for a post-doctoral fellowship (G.T.M.S.).

References

1. Pina F (2014) Chemical applications of anthocyanins and related compounds. A source of bioinspiration. J Agric Food Chem 62:6885–6897
2. Mattioli R, Francioso A, Mosca L, Silva P (2020) Anthocyanins: a comprehensive review of their chemical properties and health effects on cardiovascular and neurodegenerative diseases. Molecules 25:3809. https://doi.org/10.3390/molecules25173809
3. Quina FH, Moreira PF, Vautier-Giongo C et al (2009) Photochemistry of anthocyanins and their biological role in plant tissues. Pure Appl Chem 81:1687–1694. https://doi.org/10.1351/Pac-Con-08-09-28
4. Pina F, Oliveira J, De Freitas V (2015) Anthocyanins and derivatives are more than flavylium cations. Tetrahedron 71:3107–3114. https://doi.org/10.1016/j.tet.2014.09.051
5. Castañeda-Ovando A, Pacheco-Hernández ML, Páez-Hernández ME et al (2009) Chemical studies of anthocyanins: a review. Food Chem 113:859–871. https://doi.org/10.1016/j.foodchem.2008.09.001
6. Dangles O, Fenger J-A (2018) The chemical reactivity of anthocyanins and its consequences in food science and nutrition. Molecules 23:1970. https://doi.org/10.3390/molecules23081970
7. Basílio N, Pina F (2016) Chemistry and photochemistry of anthocyanins and related compounds: a thermodynamic and kinetic approach. Molecules 21:1502. https://doi.org/10.3390/molecules21111502
8. Quina FH, Bastos EL (2018) Chemistry inspired by the colors of fruits, flowers and wine. An Acad Bras Cienc 90:681–695. https://doi.org/10.1590/0001-3765201820170492
9. Moreira PF, Giestas L, Yihwa C et al (2003) Ground- and excited-state proton transfer in anthocyanins: from weak acids to superphotoacids. J Phys Chem A 107:4203–4210. https://doi.org/10.1021/jp027260i
10. Freitas AA, Silva CP, Silva GTM et al (2018) Ground- and excited-state acidity of analogs of red wine pyranoanthocyanins. Photochem Photobiol 94:1086–1091. https://doi.org/10.1111/php.12944
11. Alejo-Armijo A, Parola AJ, Pina F (2019) pH-dependent multistate system generated by a synthetic furanoflavylium compound: an ancestor of the anthocyanin multistate of chemical species. ACS Omega 4:4091–4100. https://doi.org/10.1021/acsomega.8b03696
12. Alejo-Armijo A, Basílio N, Freitas AA et al (2019) Ground and excited state properties of furanoflavylium derivatives. Phys Chem Chem Phys 21:21651–21662. https://doi.org/10.1039/c9cp04917g
13. Sinopoli A, Calogero G, Bartolotta A (2019) Computational aspects of anthocyanidins and anthocyanins: a review. Food Chem 297:1248. https://doi.org/10.1016/j.foodchem.2019.05.172
14. Marcano E (2017) DFT study of anthocyanidin and anthocyanin pigments for dye-sensitized solar cells: electron injecting from the excited states and adsorption onto TiO2 (anatase) surface. Phys Sci Rev 2:8. https://doi.org/10.1515/psr-2017-0008
15. Wang J, Siddique F, Freitas AA et al (2020) A computational study of the ground and excited state acidities of synthetic analogs of red wine pyranoanthocyanins. Theor Chem Acc 139:117. https://doi.org/10.1007/s00214-020-02633-9
16. Phan K, De Meester S, Raes K et al (2021) A comparative study on the photophysical properties of anthocyanins and pyranoanthocyanins. Chem A Eur J 27:1–17. https://doi.org/10.1002/chem.202004639
17. León-Carmona JR, Galano A, Alvarez-Idaboy JR (2016) Deprotonation routes of anthocyanidins in aqueous solution, pKa values, and speciation under physiological conditions. RSC Adv 6:53421–53429. https://doi.org/10.1039/c6ra10818k
18. Siddique F, Silva CP, Silva GTM et al (2019) The electronic transitions of analogs of red wine pyranoanthocyanin pigments. Photochem Photobiol Sci 18:45–53. https://doi.org/10.1039/C8PP00391B
19. Aqdas A, Siddique F, Nieman R et al (2019) Photoacidity of the 7-hydroxyflavylium cation. Photochem Photobiol 95:1339–1344. https://doi.org/10.1111/php.13139
20. Becke AD (1993) Density-functional thermochemistry. III. The role of exact exchange. J Chem Phys 98:5648–5652. https://doi.org/10.1063/1.464913
21. Grimme S, Antony J, Ehrlich S, Krieg H (2010) A consistent and accurate ab initio parametrization of density functional dispersion correction (DFT-D) for the 94 elements H-Pu. J Chem Phys 132:15104. https://doi.org/10.1063/1.3382344
22. Schäfer A, Horn H, Ahlrichs R (1992) Fully optimized contracted Gaussian basis sets for atoms Li to Kr. J Chem Phys 97:2571–2577. https://doi.org/10.1063/1.463096
23. Schäfer A, Huber C, Ahlrichs R (1994) Fully optimized contracted Gaussian basis sets of triple zeta valence quality for atoms Li to Kr. J Chem Phys 100:5829–5835. https://doi.org/10.1063/1.467146
24. Gaussian 09, Revision A.02, Frisch MJ, Trucks GW, Schlegel HB, Scuseria GE, Robb MA, Cheeseman JR, Scalmani G, Barone V, Petersson GA, Nakatsuji H, Li X, Caricato M, Marenich A, Bloino J, Janesko BG, Gomperts R, Mennucci B, Hratchian HP, Ortiz JV, Izmaylov AF, Sonnenberg JL, Williams-Young D, Ding F, Lipparini F, Egidi F, Goings J, Peng B, Petrone A, Henderson T, Ranasinghe D, Zakrzewski VG, Gao J, Rega N, Zheng G, Liang W, Hada M, Ehara M, Toyota K, Fukuda R, Hasegawa J, Ishida M, Nakajima T, Honda Y, Kitao O, Nakai H, Vreven T, Throssell K, Montgomery JA Jr, Peralta JE, Ogliaro F, Bearpark M, Heyd JJ, Brothers E, Kudin KN, Staroverov VN, Keith T, Kobayashi R, Normand J, Raghavachari K, Rendell A, Burant JC, Iyengar SS, Tomasi J, Cossi M, Millam JM, Klene M, Adamo C, Cammi R, Ochterski JW, Martin RL, Morokuma K, Farkas O, Foresman JB, Fox DJ (2016) Gaussian, Inc., Wallingford CT

25. Miertuš S, Scrocco E, Tomasi J (1981) Electrostatic interaction of a solute with a continuum. A direct utilization of AB initio molecular potentials for the prevision of solvent effects. Chem Phys 55:117–129. https://doi.org/10.1016/0301-0104(81)85090-2
26. Amovilli C, Barone V, Cammi R et al (1999) Recent advances in the description of solvent effects with the polarizable continuum model. Adv Quantum Chem 32:227–261
27. Miertuš S, Tomasi J (1982) Approximate evaluations of the electrostatic free energy and internal energy changes in solution processes. Chem Phys 65:239–245. https://doi.org/10.1016/0301-0104(82)85072-6
28. Plasser F TheoDORE: a package for theoretical density, orbital relaxation, and exciton analysis. http://theodore-qc.sourceforge.net
29. Plasser F (2020) TheoDORE: a toolbox for a detailed and automated analysis of electronic excited state computations. J Chem Phys 152:084108. https://doi.org/10.1063/1.5143076
30. Martin RL (2003) Natural transition orbitals. J Chem Phys 118:4775–4777. https://doi.org/10.1063/1.1558471
31. Gorelsky SI, Lever ABP (2001) Electronic structure and spectra of ruthenium diimine complexes by density functional theory and INDO/S. Comparison of the two methods. J Organomet Chem 635:187–196
32. Rohatgi A. WebPlotDigitizer. https://automeris.io/WebPlotDigitizer/index.html. Accessed 30 Mar 2021.

Publisher's Note Springer Nature remains neutral with regard to jurisdictional claims in published maps and institutional affiliations.